

RESEARCH ARTICLE OPEN ACCESS

Techno-Economic and Environmental Assessment of Magnesium-Impregnated Rice Husk Biochar for Nutrient Removal: A Scale-Up and Prospective Soil Application Approach

José Lugo-Arias¹  | Jose Villa-Parejo²  | Guido Escorcía³ | Elkyn Lugo-Arias⁴  | Sandra Vargas⁵  | Julia González-Álvarez⁶ 

¹Department of Civil and Environmental, Universidad de la Costa, Barranquilla, Colombia | ²Universidad del Magdalena, Santa Marta, Magdalena, Colombia | ³Faculty of Engineering, Universidad del Magdalena, Santa Marta, Magdalena, Colombia | ⁴Faculty of Economic and Business Sciences, Corporación Universitaria Minuto de Dios, UNIMINUTO, Barranquilla, Colombia | ⁵Faculty of Agricultural Sciences, Cundinamarca University, Girardot, Colombia | ⁶Department of Chemical Engineering, School of Engineering, Universidade de Santiago de Compostela, Santiago, Spain

Correspondence: Julia González-Álvarez (julia.gonzalez@usc.es)

Received: 20 November 2025 | **Revised:** 9 May 2026 | **Accepted:** 19 May 2026

Keywords: adsorption | biochar | environmental analysis | magnesium-impregnated rice husk | soil amendment | techno-economic analysis

ABSTRACT

This study evaluates the techno-economic and environmental performance of a sequential system based on fixed-bed column adsorption using magnesium-impregnated rice husk biochar (RHB-Mg) for nutrient removal from wastewater, coupled with a prospective assessment of its reuse as a soil amendment in irrigated rice systems. Scale-up based on laboratory data resulted in a treatment capacity of 4.32 m³/day and a biochar requirement of 56.91 kg/day. The system effectively reduced nitrate and phosphate concentrations below regulatory limits under continuous operation, demonstrating high adsorption performance. The techno-economic analysis over a 20-year period revealed that operational costs are primarily driven by magnesium chloride consumption, which strongly influences overall economic feasibility. Life cycle assessment (LCA) identified biochar production as the main environmental hotspot, contributing the highest impacts across multiple categories due to energy demand. Furthermore, literature-supported and LCA-based evidence indicates that the reuse of nutrient-enriched biochar could potentially reduce fertilizer demand (prospective scenario), decrease irrigation requirements, and contribute to a potential climate change benefit through carbon storage, with an estimated reduction of −1.34 kg CO₂ eq per kg of RHB-Mg applied to soil. However, this stage was evaluated as a prospective scenario and was not experimentally validated. Overall, the proposed system demonstrates strong potential within a circular-economy framework; however, process optimization—particularly in reagent consumption and energy integration—is required to enhance large-scale sustainability and economic viability.

1 | Introduction

Biochar is a carbonaceous material produced through the pyrolysis of biomass and has emerged as a promising solution for

environmental remediation and agricultural sustainability. In particular, the impregnation of biochar with magnesium (Mg) has been shown to enhance its physicochemical properties, improving its ability to remove nutrients from contaminated water

This paper presents an integrated evaluation of a magnesium-impregnated rice husk biochar system for wastewater nutrient removal and its reuse in rice cultivation. The study combines experimental data, process design, techno-economic assessment, and life-cycle analysis to determine system efficiency, environmental impacts, and scalability, emphasizing optimization strategies to enhance circular-economy performance.

This is an open access article under the terms of the [Creative Commons Attribution-NonCommercial-NoDerivs](https://creativecommons.org/licenses/by-nc-nd/4.0/) License, which permits use and distribution in any medium, provided the original work is properly cited, the use is non-commercial and no modifications or adaptations are made.

© 2026 The Author(s). *Water Environment Research* published by Wiley Periodicals LLC on behalf of Water Environment Federation.

Summary

- Magnesium-modified rice husk biochar effectively removes nitrate and phosphate from wastewater in fixed-bed operation.
- Spent biochar can be safely reused as a soil amendment, improving agronomic performance in rice cultivation.
- Magnesium chloride cost is the primary barrier limiting large-scale economic feasibility of the treatment system.
- Life-cycle assessment shows biochar preparation drives most environmental burdens, requiring energy and reagent optimization.
- Integrating nutrient recovery and soil reuse enhances circular-economy potential in agricultural wastewater management.

and potentially contributing to soil amendment applications (Peng et al. 2023; Blanco-Canqui 2017). These applications are particularly relevant in regions with intensive agricultural systems, such as rice cultivation, where nutrient management and soil improvement represent persistent challenges.

However, the application of biochar derived from different biomass sources without chemical modification has shown limited effectiveness for nutrient adsorption. This is mainly due to the negatively charged surface of both the adsorbent and the primary target nutrients present in wastewater and agricultural runoff, which are typically found as anionic species such as nitrate and phosphate, leading to electrostatic repulsion and consequently low or negligible adsorption capacities (Pratiwi et al. 2016). Therefore, chemical modification using elements such as magnesium (Mg) has been widely investigated to enhance the adsorption properties of pristine biochars, including those derived from rice husk and other precursors.

The use of RHB-Mg can improve nutrient adsorption through multiple mechanisms, as reported in previous studies, thereby increasing the removal efficiency of nitrates and phosphates. For instance, the incorporation of Mg-based functional groups (e.g., MgO and Mg(OH)₂), resulting from MgCl₂ impregnation, may provide several advantages (Lugo-Arias et al. 2026; Tran et al. 2022; Biswas et al. 2024): (1) enhanced electrostatic attraction between the adsorbent and anionic nutrients due to an increase in the point of zero charge, enabling the biochar surface to become positively charged at near-neutral pH conditions typical of many wastewaters; (2) ion exchange interactions with Mg-derived cations present in RHB-Mg; (3) precipitation of phosphate species such as Mg(H₂PO₄)₂, MgHPO₄, and Mg₃(PO₄)₂; and (4) complexation of phosphorus with surface functional groups (e.g., C=O and -OH), further enhancing phosphate removal. In contrast, nitrate removal is generally attributed to weaker interactions such as electrostatic attraction and ion exchange, which may be more sensitive to water chemistry conditions. It is important to note that these mechanisms are proposed based on previously reported characterization and literature evidence and were not directly verified in the present study through postadsorption analyses. Therefore, further

investigation using techniques such as XRD, FTIR, SEM-EDS, or desorption tests is required to confirm the dominant removal pathways, particularly for nitrate.

Recent studies have highlighted the ability of magnesium-impregnated biochar to efficiently adsorb these specific ions through both chemical and physical adsorption processes (Tran et al. 2022; Zhang et al. 2024; Chen et al. 2024). By capturing nitrate and phosphate, this approach may contribute to mitigating eutrophication and enabling nutrient recovery; however, these applications are often evaluated separately. Moreover, the use of biochar in agriculture has been associated with improvements in soil properties such as water retention capacity, nutrient availability, and structural stability, which may support crop productivity and long-term soil sustainability (Blanco-Canqui 2017).

From a technical and economic standpoint, the production of magnesium-impregnated biochar requires a detailed analysis of the costs and benefits associated with its production and its dual application—first for the decontamination of nutrient-enriched water, and subsequently for soil improvement. Previous studies have highlighted the need to optimize processes such as pyrolysis and chemical impregnation to significantly reduce operational and capital costs, thereby enhancing the feasibility of large-scale implementation (Peng et al. 2023; Jellali et al. 2024; Ighalo et al. 2022; Sivaraman et al. 2024). Additionally, the incorporation of circular-economy principles—such as nutrient recovery and the valorization of agricultural residues—adds an environmentally sustainable dimension to biochar utilization (Peng et al. 2023).

Despite the well-documented benefits of biochar, its overall environmental performance remains highly context dependent. Several studies have identified important trade-offs associated with its production, particularly due to the energy-intensive nature of pyrolysis (Chen et al. 2024; Moreira et al. 2017), which can offset carbon sequestration benefits if not properly optimized (Lugo-Arias, Villa-Parejo, et al. 2025). For example, high energy demand and reliance on nonrenewable energy (NRE) sources during biochar production may lead to substantial greenhouse gas emissions, thereby diminishing the net environmental advantage of the system. These limitations highlight the need for integrated evaluation frameworks that simultaneously consider technical performance, economic feasibility, and environmental impacts, including full life cycle implications, particularly when proposing circular-economy strategies involving the reuse of spent biochar in agricultural applications.

However, there remains a lack of studies that simultaneously evaluate fixed-bed column performance, scale-up requirements, and the combined techno-economic and life cycle impacts of RHB-Mg systems, particularly within circular economy frameworks that link wastewater treatment with subsequent agricultural reuse.

To clearly distinguish the scope of this work, it is important to note that the adsorption performance and physicochemical characterization of RHB-Mg have been previously reported by the authors. Therefore, this study does not provide new experimental adsorption data, but instead develops a system-level evaluation based on previously validated results.

Accordingly, the main novelty of this work lies in the integration of (i) scale-up analysis of a fixed-bed adsorption system, (ii) techno-economic assessment (TEA), (iii) life cycle assessment (LCA), and (iv) a prospective evaluation of the reuse of nutrient-loaded biochar as a soil amendment within a circular-economy framework.

The objective of this study is to evaluate the production and application of RHB-Mg from a techno-economic and environmental perspective, with a primary focus on its performance for nutrient removal in wastewater treatment systems. Additionally, the reuse of nutrient-loaded biochar is assessed as a prospective scenario based on literature data and life cycle modeling, rather than direct experimental validation.

This approach explores the feasibility of integrating RHB-Mg-based adsorption systems within a circular economy framework, but does not represent a fully validated operational system at pilot or industrial scale. The reuse of treated wastewater (e.g., for irrigation) was not considered in this study and should be addressed in future assessments to further strengthen the circular-economy potential of the system.

In alignment with global sustainability priorities, this research discusses potential contributions to several United Nations Sustainable Development Goals (SDGs) through measurable and practical outcomes. Specifically, the proposed system may contribute to SDG 6 (Clean Water and Sanitation) by enabling the removal of nitrates and phosphates to meet regulatory discharge limits, and may contribute to SDG 12 (Responsible Consumption and Production) by valorizing agricultural residues such as rice husk and promoting nutrient recovery. Furthermore, the reuse of nutrient-enriched biochar in soil may support SDG 2 (Zero Hunger) by enhancing soil fertility and potentially improving crop productivity. From a climate perspective, the system may contribute to SDG 13 (Climate Action) through carbon sequestration and the reduction of greenhouse gas emissions associated with fertilizer use and irrigation. Therefore, these contributions are interpreted as potential outcomes based on system-level analysis and should be validated through future experimental and field-scale studies. For clarity, the distinction between previously published data and new contributions is summarized in Table 1.

The performance of biochar-based systems depends strongly on the physicochemical characteristics of the raw biomass, the modification methods, and the application conditions, rather than on

biochar as a generic material (Osman, Fawzy, et al. 2022). In this context, this study adopts a structure–property–performance–environment perspective to interpret the RHB-Mg system.

The effects of $MgCl_2$ impregnation on the surface chemistry of biochar and its adsorption behavior have been widely reported in the literature; however, these relationships were not experimentally evaluated in this work and are considered based on previous studies conducted by the authors. Accordingly, $MgCl_2$ loading is assumed to be directly linked to adsorption performance and, consequently, to reagent consumption, thereby influencing both economic and environmental outcomes.

Furthermore, the performance of spent biochar when applied to soil depends on nutrient retention and leaching behavior, which were not evaluated in this study and therefore introduce uncertainty into the system-level assessment.

2 | Experimental Section

2.1 | Scaling of the Adsorption Process

The scaling of the coadsorption process for nitrates and phosphates was carried out using experimental data obtained from fixed-bed column adsorption tests at a small scale, which are summarized in Table S1. The physicochemical characterization results of RHB-Mg, as well as the fixed-bed adsorption experiments, have been previously reported by the authors (Lugo-Arias et al. 2026). Additional details on the physicochemical properties of RHB-Mg can be found in related studies by the same authors (Lugo-Arias et al. 2026; Lugo-Arias, González-Álvarez, et al. 2025). Regarding the reuse of the spent adsorbent, it is important to note that parameters related to the long-term stability of biochar in soil, such as the H/C ratio, were not evaluated in this study, as no experimental soil application was conducted. Instead, the assessment of biochar reuse was based on a literature review and LCA.

The scaling equations were based on formulations proposed in other studies (Jellali et al. 2024; Bian et al. 2024; Jung et al. 2017), with the aim of upscaling to a flow rate of 0.05 L/s (4.32 m³/day), which is consistent with the values used in several scaling studies (Esmati et al. 2024). In the present research, the bed height was kept constant at H=8 cm, as this was the optimal value obtained in previous experiments, yielding the best dual-solute

TABLE 1 | Distinction between previously published data and new contributions.

Component	Source
Adsorption performance of RHB-Mg	Previously published by the authors
Physicochemical characterization	Previously published by the authors
Fixed-bed experimental data	Previously published by the authors
Scale-up	This study
Techno-economic assessment (TEA)	This study
LCA	This study
Soil application scenario	Literature-based (prospective)

adsorption performance for nitrates and phosphates from real wastewater using RHB-Mg.

The adsorption rate (FR) of the circular column geometry was calculated using Equation (1):

$$FR = \frac{Q_{ss}}{A_{ss}} = \frac{4Q_{ss}}{\pi D_{ss}^2} \quad (1)$$

where Q_{ss} is the small-scale column flow rate and A_{ss} is the cross-sectional area of the small-scale column.

Assuming that the adsorption rate (FR) remains constant during scale-up, the cross-sectional area of the large-scale column (A_{LS}) can be expressed as a function of the operating flow rate using Equation (2):

$$A_{LS} = \frac{Q_{LS}}{FR} \quad (2)$$

where Q_{LS} is the flow rate of the large-scale column. Based on this relationship given in Equation (2), the bed volume of the large-scale column ($V_{b,LS}$) was determined from the column geometry, as shown in Equation (3):

$$V_{b,LS} = A_{LS}H_{LS} \quad (3)$$

where H_{LS} is the depth or height of the bed in the large-scale column.

The hydraulic retention time (HRT) in the column was estimated considering $V_{b,LS}$ from Equation (3) and the volumetric flow rate relationship, resulting in Equation (4):

$$HRT = \frac{V_{b,LS}}{Q_{LS}} \quad (4)$$

The mass of adsorbent in the large-scale column (m_a) was obtained using Equation (5):

$$m_a = (\rho_{biochar})(V_{b,LS}) \quad (5)$$

where ρ is the density of the biochar.

The breakthrough volume ($V_{br,LS}$), which is the amount of water treated before breakthrough, for each contaminant in the large-scale column was determined using Equation (6):

$$V_{br,LS} = (Q_{LS})(t_b) \quad (6)$$

where t_b represents the breakthrough time for either nitrates or phosphates, depending on the contaminant being analyzed.

Based on this definition and the relationship given in Equation (6), the service time of the column (t_B) of the large-scale column can be expressed as shown in Equation (7):

$$t_B = \frac{V_{br,LS}}{Q_{LS}} \quad (7)$$

By substituting the expression for the breakthrough volume, it follows that $t_B = t_b$, indicating that, under the defined operating conditions, the service time of the column is equivalent to the breakthrough time.

Estimates for the requirements of equipment, materials, and operational variables—both for pyrolysis and soil application—were based on the quantities of RHB-Mg required for the adsorption process (see [Supporting Information](#)).

The process flow diagrams are summarized in Figure 1, while the operating conditions and adsorbent preparation details are specified in the [Supporting Information](#).

It should be noted that the scale-up approach adopted in this study is based on maintaining superficial velocity and bed height as a first approximation. Therefore, the results should be interpreted as preliminary design estimates. Advanced fixed-bed modeling approaches (e.g., BDST, Thomas, Yoon–Nelson) and pilot-scale validation were not included in this study and are recommended for future work to improve the robustness of the design.

2.2 | Techno-Economic Analysis (TEA)

2.2.1 | Estimation of Total Capital Costs

The cost of preparing the adsorbent and operating the adsorption column was calculated based on the total capital investment (TCI), as expressed in Equation (8) (Gopalakrishnan et al. 2020):

$$TCI = WCC + FCE \quad (8)$$

where WCC represents the working capital cost and FCE the fixed-capital estimate.

2.2.2 | Estimation of Annual Operating Cost

The annual operating cost (AOC) for adsorbent preparation was determined using Equation (9) (Gopalakrishnan et al. 2020):

$$AOC = C_{RM} + C_{WG} + C_U + C_E \quad (9)$$

where C_{RM} is the cost of raw materials, C_{WG} is the cost of handling waste generated during operation, C_U is the cost of public services (e.g., energy, water), and C_E is the additional costs.

The unit cost of the produced adsorbent (C_e) was calculated from the AOC and the annual production of adsorbent (E_p) using Equation (10) (Ighalo et al. 2022):

$$C_e = \frac{AOC}{E_p} \quad (10)$$

The energy costs (C_{ene}) were estimated using Equation (11) (El-Shafie et al. 2024):

$$C_{ene} = H * MP * COEY \quad (11)$$

where H is the number of hours of equipment operation, MP is the maximum power of the equipment (kW), and $COEY$ is the unit cost of electrical energy (COP/kWh).

The pump power required (P) to drive the water flow through the column was calculated using Equation (12) (Saldarriaga 2016):

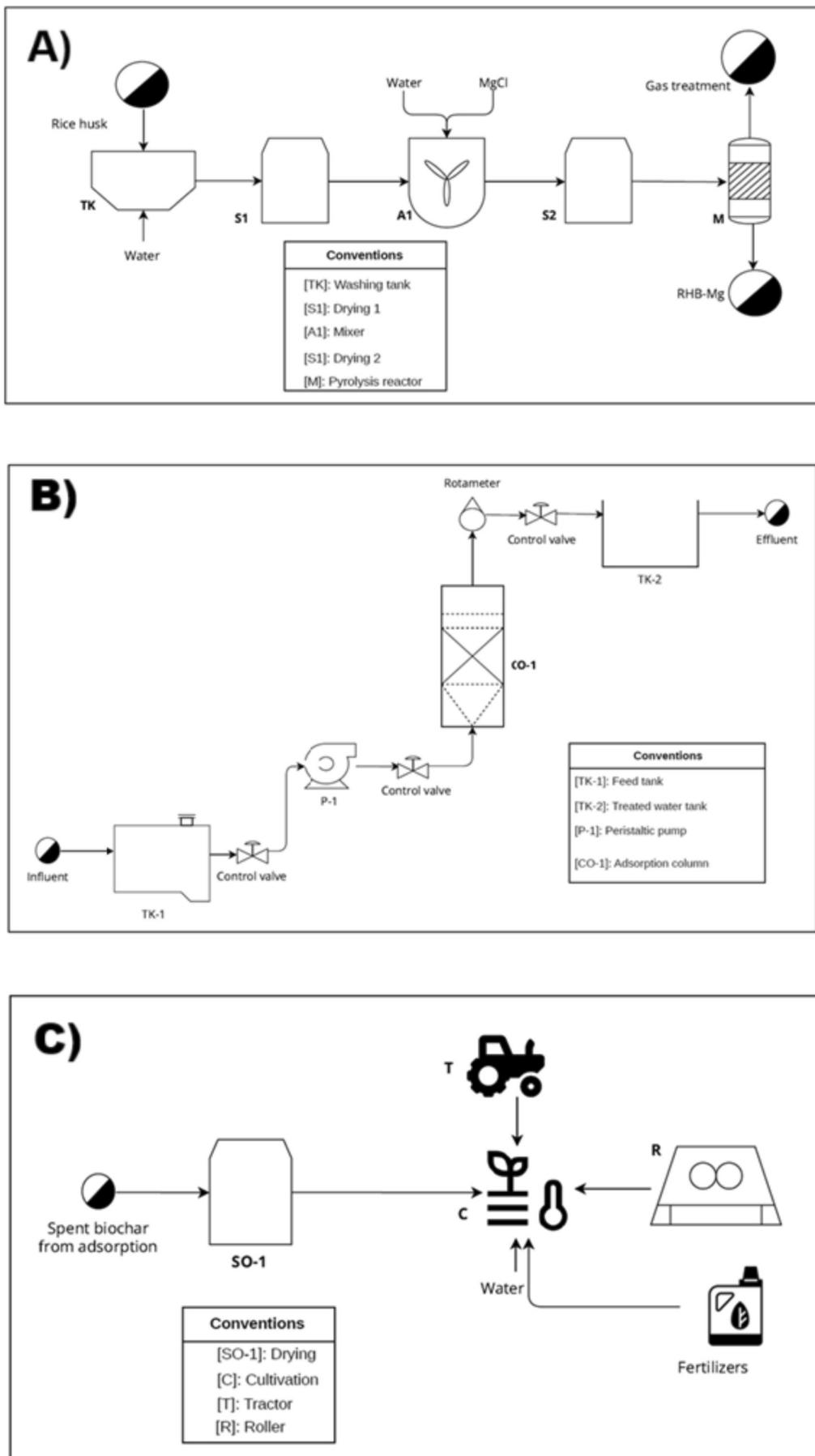


FIGURE 1 | Process diagrams for the application of RHB-Mg: (A) biochar production, (B) adsorption, and (C) soil application.

$$P = \frac{1}{\eta} \rho g Q H_{DT} \quad (12)$$

where Q is the flow rate (m^3/s), ρ is the water density (kg/m^3), η is the pump efficiency (dimensionless), and H_{DT} is the total dynamic head or energy required by the pump ($\text{N}\cdot\text{m}/\text{N}$).

The total dynamic head was estimated from the general energy equation for pipeline systems (Equation 13) (Saldarriaga 2016):

$$H_{DT} = H_{est} + \left(\sum K_{ms} \frac{1}{D_s^4} + f_s \frac{L_s}{D_s^5} + \sum K_{mi} \frac{1}{D_i^4} + f_i \frac{L_i}{D_i^5} \right) \frac{8Q^2}{g\pi^2} + \frac{\Delta P}{\gamma} \quad (13)$$

where H_{est} is the height difference between influent and effluent reservoirs (m), $\sum K_{ms}$ and $\sum K_{mi}$ are the global loss coefficients in suction and discharge pipes (dimensionless), L_s and L_i are respective lengths of the suction and discharge pipes (m), D_s and D_i are respective diameters of the suction and discharge pipes (m), f_s and f_i are friction factors of the suction and discharge pipes, respectively (dimensionless, calculated via the Colebrook-White equation), γ is the specific weight of water (N/m^3), and ΔP is the pressure drop (Pa), calculated using the Ergun equation (Equation 14) (Kumar et al. 2019):

$$\Delta P = \left[\frac{150 * \mu * L * (1 - \epsilon)^2 * v}{(D_p)^2 * (\epsilon)^3} \right] + \left[\frac{1.75 * L * \rho * (1 - \epsilon) * (v)^2}{D_p * (\epsilon)^3} \right] \quad (14)$$

where μ is the dynamic viscosity of the fluid ($\text{kg}/\text{m}\cdot\text{s}$), L is the length of the packed bed (m), v is the superficial velocity (m/s), D_p is the particle diameter (m), ϵ is the void fraction of the bed, and ρ is the fluid density (kg/m^3).

The cost of applying nutrient-loaded RHB-Mg to soil (CAS) was determined using Equation (15) (Patel and Panwar 2024):

$$CAS = CT + CO - CP - C \quad (15)$$

where CT is the transport costs, CO is the operating costs, CP is the loss costs, and C is the revenues generated.

2.2.3 | TEA Indicator

The net present value (NPV) was used as the main TEA indicator, calculated according to Equation (16):

$$NPV = \sum_{t=1}^n \frac{I_t - C_t}{(1+i)^t} - I_0 \quad (16)$$

where I_0 is the initial capital investment, i is the discount rate, n is the total number of years, and I_t and C_t are the revenues and costs in year t , respectively. The tax rate and interest rate were set at 35% and 12.75%, respectively, in accordance with the Colombian financial context (Alonso-Gómez et al. 2024). A process lifetime of 20 years was assumed (Esmati et al. 2024).

2.3 | LCA

The LCA was conducted following the methodology defined by the ISO 14040 and ISO 14044 standards, applying the four phases: definition of goal and scope, life cycle inventory (LCI), environmental impact assessment, and interpretation of results.

2.3.1 | Goal and Scope of the Study

The objective of this research is to determine the environmental performance of the application of RHB-Mg in the co-adsorption of nitrates and phosphates from wastewater under a fixed-bed column operation mode. Additionally, the reuse of nutrient-loaded biochar for improving soil properties in irrigated rice cultivation is assessed as a prospective scenario, supported by literature and LCA results within the Colombian context.

A cradle-to-grave approach was applied, with a functional unit of 1 kg of biochar produced, as illustrated in Figure 2. While this functional unit is appropriate for evaluating the environmental burdens associated with the production of RHB-Mg, it does not directly reflect treatment performance or the nutrient recovery efficiency of the adsorption process. Therefore, complementary performance-based indicators were derived from the system-scale results to improve interpretability and enable comparison with wastewater treatment technologies. These were normalized to the production of 1 kg of RHB-Mg, based on a production rate of 56.91 kg of RHB-Mg and nutrient removals of 21.16 g/day for nitrate and 12.1 g/day for phosphate, without modifying the underlying LCI. The resulting normalized values correspond to 0.03789 m^3 of treated wastewater per kg of RHB-Mg, 0.3718 g of NO_3^- removed per kg of RHB-Mg, and 0.2126 g of PO_4^{3-} removed per kg of RHB-Mg. This approach is consistent with recent LCA studies on adsorbents, which emphasize the need to link functional units to process performance (e.g., adsorption and soil application) (Osman, Elgarahy, et al. 2022; Osman et al. 2024).

With respect to soil application, a functional unit based on 1 ha of rice cultivation was not implemented due to the prospective nature of the soil application stage. However, the calculations for the application of spent RHB-Mg were based on a dosage of 18-t RHB-Mg per hectare, as reported in the literature, although normalization to this functional unit will require further investigation.

2.3.2 | LCI

The LCI of biochar production and application processes was developed using mass and energy balance calculations. The results are summarized in Table 2.

The processes were modeled using the European Reference Life Cycle Database (ELCD) incorporated into the OpenLCA 2.2 software, which enabled conversion of the inventory data into environmental impacts.

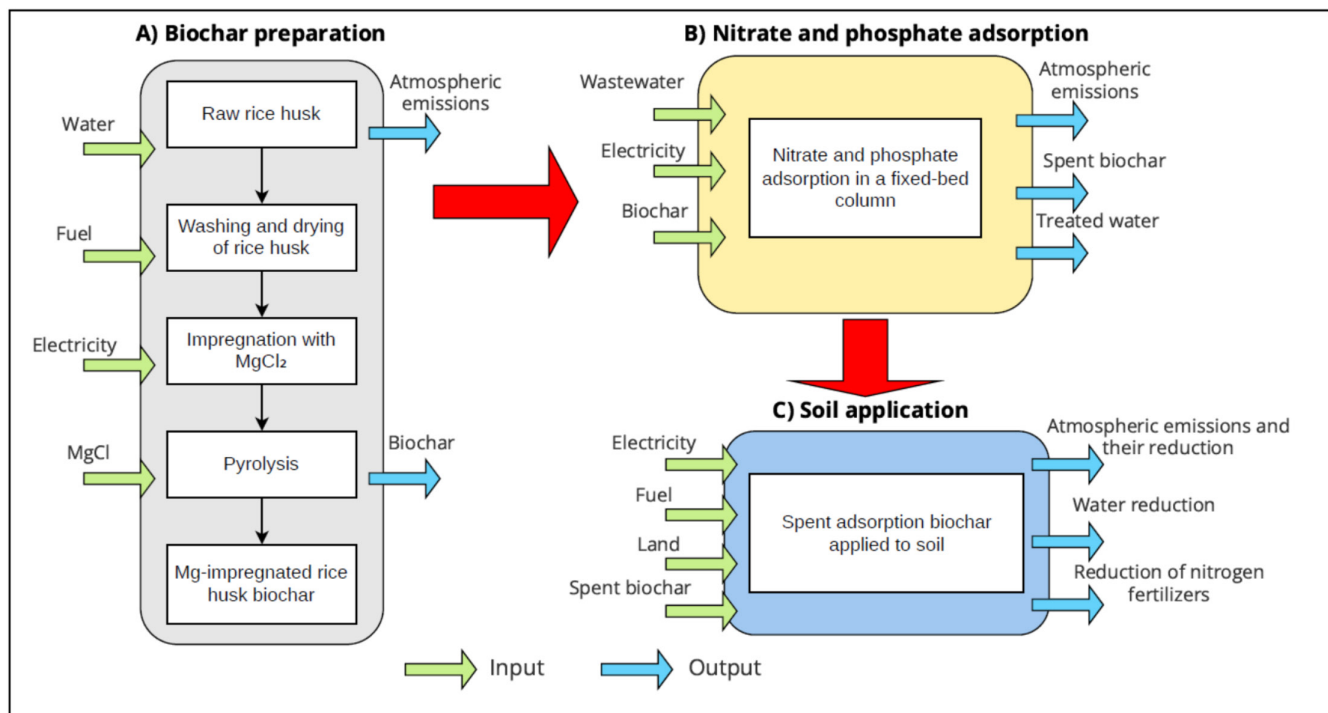


FIGURE 2 | System boundaries for the biochar application process.

All detailed calculations for the LCI can be found in Appendix S2.

The $MgCl_2$ input reported in this study was estimated based on impregnation protocols derived from the literature and should be interpreted as a process assumption intended to ensure the formation of Mg-based functional groups, rather than as a fully validated material balance. Although the stoichiometric calculations are internally consistent, the fate of Mg and chloride throughout the process (including impregnation, washing, drying, adsorption, and effluent streams) was not explicitly tracked.

Therefore, key aspects such as Mg retention efficiency, residual chloride content in RHB-Mg, the composition of washing effluents, and the potential release of Mg or Cl during operation remain uncertain. As a result, the reported $MgCl_2$ consumption may represent a conservative estimate, and its contribution to environmental impacts should be interpreted with caution.

Future studies should include a detailed mass balance of Mg and chloride to evaluate process efficiency, identify potential losses, and assess the environmental implications associated with reagent use and effluent generation.

2.3.3 | Environmental Impact Assessment

The environmental impacts of the processes associated with the application of RHB-Mg were assessed using the IMPACT 2002+ method, which is widely applied to biochar systems (Rajabi Hamedani et al. 2019).

This method considers 14 environmental impact categories (Joliet et al. 2003), encompassing climate change, toxicity, resource depletion, and ecosystem impacts.

2.3.4 | Sensitivity Analysis

Regarding the sensitivity analysis, Colombia's main electricity generation source (hydropower) was compared with two alternative energy sources: wind energy and energy derived from synthesis gas (syngas), generated during the thermochemical decomposition of biomass through the pyrolysis process. This comparison enabled the evaluation of variations in the environmental impacts associated with replacing the hydropower-based energy matrix with alternative energy sources across the same impact categories, with the aim of identifying the options with the best environmental performance and greatest sustainability.

3 | Results and Discussion

3.1 | Scaling of the System

3.1.1 | Scaling of the Adsorption Process

The scaling design was carried out following the methodology described in Section 2.1. Based on the selected operating conditions (Table S2), the system was designed to treat a flow rate of $4.32 \text{ m}^3/\text{day}$. This resulted in a column diameter of 43.44 cm and a hydraulic retention time (HRT) of approximately 4 min. Under these conditions, the process is expected to achieve effluent concentrations below the regulatory limits established in Colombia for nitrates (10 mg/L) and phosphates (0.5 mg/L).

TABLE 2 | Life cycle inventory of the biochar application process.

Stage	Inputs				Outputs			
	Variable	Quantity	Unit	Source	Variable	Quantity	Unit	Source
(A) Biochar preparation	Rice husk	2	kg	Created	Transported husk	2	kg	Created
	Transport	2×20	t-km	ELCD	Mg-treated husk	2	kg	Created
	Tap water	36.6	L	ELCD	CH ₄ emissions	0.0114	kg CH ₄	ELCD
	Electricity	0.61	kWh	ELCD	NO _x emissions	0.00074	kg NO _x	ELCD
	MgCl ₂	20	kg	ELCD	PM ₁₀ emissions	0.00154	kg PM ₁₀	ELCD
	Drying area	0.17	m ²	ELCD	RHB-Mg	1	kg	ELCD
(B) Adsorption of nitrates and phosphates in fixed-bed column	Mg-treated husk	2	kg	Created	—	—	—	—
	Electricity	0.078	kWh	ELCD	Treated water	37.89	L	ELCD
	Wastewater	37.89	L	ELCD	Spent RHB-Mg	1	kg	Created
(C) Soil application	RHB-Mg	1	kg	Created	—	—	—	—
	Spent RHB-Mg	1	kg	Created	Reduction in nitrogen fertilizer use	-0.00353	kg N	ELCD
	Drying area	0.17	m ²	ELCD	Reduction in CH ₄ emissions	-35	kg CH ₄	ELCD
	Application area	0.555	m ²	ELCD	Reduction in N ₂ O emissions	-0.72	kg N ₂ O	ELCD
	Tractor use (disc plow, sprayer, and roller)	0.02	min	ELCD	Reduction in irrigation water use	-160	L	ELCD
	RHB-Mg transport	20	t-km	ELCD	CO ₂ capture	-1.34762	kg CO ₂	ELCD

The service time for the coadsorption of nitrates and phosphates was 1 h, corresponding to the nitrate breakthrough time (shorter than the approximately 4 h required for phosphate saturation). Nitrate was therefore identified as the limiting nutrient, because its concentration would exceed the water quality standards during extended operation (El-Shafie et al. 2024).

This difference in breakthrough behavior has important implications for both process performance and practical operation. Because nitrate reaches breakthrough after about 1 h, the system must be operated based on this limit, which leads to the premature termination of the adsorption cycle. As a result, a significant portion of the phosphate adsorption capacity remains unused, indicating an underutilization of the adsorbent.

In addition, the amount of nitrate removed before breakthrough is relatively low compared to the mass of adsorbent used per cycle, suggesting limited adsorbent utilization efficiency under the selected conditions. Overall, this behavior represents a key limitation of the system and highlights the need for process optimization or alternative configurations, such as multistage or selective removal approaches.

For continuous operation over 24 h, the number of cycles per day was 24, resulting in a total of 8760 cycles per year. The short nitrate breakthrough time therefore implies frequent replacement or regeneration cycles, which would be impractical under a single-column configuration. From an operational perspective, this reflects a trade-off between meeting discharge standards and maintaining efficient adsorbent utilization.

Therefore, a multicolumn system (e.g., lead-lag configuration) is required to enable continuous operation. However, this operational complexity was not explicitly modeled and should be considered in future process design and cost evaluations.

3.1.2 | Scaling of the Biochar Production Process

Table S3 summarizes the parameters used to scale up the pyrolysis process for biochar production, while detailed calculations are provided in Appendix S1. The scaling was based on the daily biochar demand required for the adsorption system, assuming that biochar production operates as a parallel unit within the overall process, together with the subsequent application of spent biochar to soil.

To meet a daily biochar requirement of 56.91 kg, a raw rice husk input of 113.82 kg was estimated, assuming a biochar yield of 0.5 relative to the initial biomass. The selected reference unit (LM-E60, ARDER, Colombia), with a 60-L capacity and a maximum power of 9 kW, would require approximately seven pyrolysis cycles per day, each with a processing time of 1 h.

Although this configuration provides a feasible first approximation for meeting the adsorbent demand, it also reveals important operational and environmental implications. In particular, the need for multiple daily pyrolysis cycles suggests a relatively energy-intensive process, which may significantly influence both the economic performance and the environmental footprint of the system, as further discussed in the TEA and LCA sections.

Additionally, the assumption of a constant biochar yield and steady operation does not account for potential variability in feedstock properties, thermal efficiency, or scale-dependent heat transfer limitations. These factors could affect both the quantity and quality of the produced biochar and consequently its adsorption performance.

Overall, these results highlight that biochar production is not only a supporting step but a critical component of the system, directly affecting its scalability, cost structure, and environmental impact.

3.1.3 | Scaling of the Spent Biochar Application Process

The application area was estimated at 1.15 ha based on the annual production of RHB-Mg (20.77 t/year) and an application rate of 18 t/ha, corresponding to the reference value reported for rice-cultivated soils (Mohammadi et al. 2016). This rate was selected to explore the potential integration of nutrient-loaded biochar within an agricultural reuse pathway.

From a system perspective, the selected application dose represents a relatively high input of material to the soil, which may enhance nutrient availability but also raises important considerations regarding long-term accumulation effects,

particularly for Mg and associated ions. In this context, the agronomic performance of the spent biochar should be interpreted as a prospective scenario rather than a validated outcome.

Although the scaling calculations indicate that the annual biochar production could be applied within a relatively limited agricultural area, the practical feasibility of this approach depends on several factors not addressed in this study. These include nutrient release dynamics, potential leaching, soil chemical changes (e.g., pH and salinity), and crop response under real field conditions.

The design parameters related to field application (e.g., plowing, dosing, and homogenization equipment) are provided in Table S4 and Appendix S1. However, these operational details are not the primary focus of the analysis and are presented only to support the system-level estimation.

3.2 | Nutrient Balance Analysis

A nutrient balance was performed to evaluate the consistency of nitrate and phosphate removal in the adsorption system using RHB-Mg. The mass balance was calculated based on influent and effluent concentrations and the system flow rate.

For nitrate, the influent load was 64.37 g/day, while the effluent load was 43.2 g/day, resulting in a removal of 21.16 g/day. In the case of phosphate, the influent load was 14.26 g/day and the effluent load was 2.16 g/day, corresponding to a removal of 12.1 g/day (Table 3).

The mass balance closure was 100% for both nutrients, indicating internal consistency of the calculations. The results confirm that phosphate removal is significantly higher than nitrate removal, which is consistent with the stronger adsorption and precipitation mechanisms associated with Mg-modified biochar, whereas nitrate removal is more limited due to weaker interaction mechanisms, as discussed in previous sections.

TABLE 3 | Nutrient balance for nitrate and phosphate at system scale.

Parameter	Nitrate	Phosphate
Influent concentration (mg/L)	14.9	3.3
Effluent concentration (mg/L)	10	0.5
Flow rate (L/day)	4320	4320
Influent load (g/day)	64.37	14.26
Effluent load (g/day)	43.2	2.16
Removed load (g/day)	21.16	12.1
Mass balance closure (%)	100	100

3.3 | TEA

3.3.1 | Estimation of Total Capital Costs

The total capital cost for the installation and equipment required for the proposed system—including biochar production, fixed-bed adsorption, and subsequent soil application—was estimated at 122,762,675 Colombian pesos (COP). This value represents the fixed and working capital investment needed to produce RHB-Mg and operate the adsorption system under the defined design conditions.

From a system perspective, this capital requirement reflects a relatively simple configuration, as it excludes additional infrastructure such as pre-treatment units or land acquisition. These elements were not considered in the present analysis because the system is assumed to be integrated into an existing wastewater treatment facility and applied within already available agricultural land.

Although the estimated capital cost provides a useful baseline, it should be interpreted with caution. The simplified system boundaries may underestimate the actual investment required under real operating conditions, particularly when considering additional process units, infrastructure, and integration requirements.

Furthermore, the capital cost must be evaluated in conjunction with operational constraints identified in the adsorption system, such as the short nitrate breakthrough time. These factors may increase equipment redundancy (e.g., multiple columns) and operational complexity, which could lead to higher capital and installation costs than those estimated in this preliminary design.

Overall, these results suggest that, while the initial capital investment appears moderate, the practical implementation of the system may require additional infrastructure and configuration adjustments that could significantly influence its economic feasibility.

3.3.2 | Estimation of Annual Operating Costs

The annual operating cost to produce RHB-Mg was estimated at COP 249,479/kg. This relatively high cost is primarily driven by the consumption of magnesium chloride, with approximately 415 tons of industrial-grade $\text{MgCl}_2 \cdot 6\text{H}_2\text{O}$ required for the impregnation of 41.44 tons of rice husk at a unit price of COP 11,783,999/t in Colombia. This finding highlights a direct relationship between material design (Mg loading) and economic performance, as the amount of MgCl_2 required to enhance adsorption directly determines reagent consumption and overall production cost.

These results indicate that reagent consumption, rather than energy or biomass supply, is the dominant cost driver in the system. The MgCl_2 consumption used in this study was based on impregnation conditions reported in the literature and was not optimized; therefore, the reported reagent demand should be interpreted as a conservative scenario. This assumption has a strong influence on both the economic and environmental

performance of the system and highlights the need for optimization strategies aimed at reducing Mg dosage while maintaining adsorption efficiency.

As a consequence, the economic performance of the process is highly sensitive to MgCl_2 price and dosage, making the current configuration economically challenging under baseline conditions. Although the cost could potentially be reduced through process optimization—such as lowering magnesium chloride concentration (3.3M in this study), improving impregnation efficiency, or adjusting pyrolysis conditions—these strategies were not evaluated in detail and remain subject to future investigation (Iamsaard et al. 2023; Fang et al. 2014; Jiang et al. 2019; Liu et al. 2022).

From a comparative perspective, the reported production costs of adsorbents in the literature range from COP 2239 to 534,322/kg (Table 4), reflecting significant variability due to differences in feedstock, energy sources, and regional price structures (Ighalo et al. 2022; El-Shafie et al. 2024). In this context, the cost obtained in this study falls within the upper range, reinforcing the need for optimization.

If MgCl_2 impregnation were omitted, the production cost would decrease substantially to COP 4458/kg. However, this scenario would compromise the adsorption performance, as unmodified rice husk biochar is not effective for the removal of negatively charged species such as nitrate and phosphate (Pratiwi et al. 2016). This highlights a key trade-off between cost reduction and functional performance.

The operational cost of the overall adsorption system, including biochar production and column operation, was estimated at COP 3,202,735/m³. This value is considerably higher than typical costs reported for conventional nutrient removal technologies, suggesting that the proposed system is not economically competitive under the current assumptions.

While alternative approaches such as direct MgCl_2 precipitation or biological treatment systems may offer lower operational costs, the use of RHB-Mg presents potential advantages, including reduced sludge generation, improved handling of solid materials, and the possibility of reusing nutrient-loaded biochar within a circular-economy framework. However, these benefits are not sufficient to offset the high reagent cost under the baseline scenario.

The application of nutrient-loaded (spent) RHB-Mg to soil was estimated at COP 864,730/ha, with potential economic savings of –COP 10,080,000/ha from reduced irrigation water use and –COP 178,112/ha from reduced nitrogen fertilizer application. In addition, indirect benefits may arise from greenhouse gas mitigation (CO_2 , CH_4 , and N_2O) (Mohammadi et al. 2016), although these were not monetized in the present analysis.

Overall, these results indicate that, despite the potential environmental and circular-economy benefits, the economic feasibility of the system is currently limited by the high consumption of magnesium chloride. Therefore, significant process optimization or alternative design strategies would be required to improve its competitiveness.

TABLE 4 | Comparison of biochar production and adsorption costs reported in the literature.

Study/technology	Feedstock or process	Target pollutant	Estimated cost (COP/kg)	Treatment cost (COP 2025/m ³)	Cost per kg nutrient removed (COP 2025/kg)	Reference
Soil amendment	Rice husk biochar	NA (soil application)	4458	NA	NA	This study
Adsorption	RHB-Mg	NO ₃ ⁻ /PO ₄ ³⁻	249,479	3,202,735	3,200,000	This study
	Rice husk biochar	Dye (Basic Red 09)	2239	NA	NA	(Praveen et al. 2021)
Biochar production (without pollutant removal)	<i>Colocasia esculenta</i> biochar	Fe ²⁺ , Cu ²⁺ , and As ⁵⁺	5239	NA	NA	(Banerjee et al. 2016)
	Neem seed biochar (with NaHCO ₃ and urea)	Magnesium and strontium ions	457,543	NA	NA	(Gariya and Satyavathi 2024)
	Olive stone biochar	Clofazimine	64,566	NA	NA	(El-Azazy et al. 2021)
Biochar production (without pollutant removal)	Magnetic olive stone biochar		534,322	NA	NA	
	Canola straw biochar	Arsenic	21,761	NA	NA	(Norberto et al. 2023)
	Maize biochar modified with Mg	PO ₄ ³⁻	26,113	NR	121,207	(Peng et al. 2023)
	Popcorn biochar modified with Mg		26,409		273,578	
Biochar production (without pollutant removal)	Sulphonated magnetic palm kernel shell biochar	NA	26,536	NA	NA	(Seow et al. 2024)
	Coconut shell biochar		13,986	NA	NA	
	Soybean straw biochar		129,513	NA	NA	
Chemical precipitation	FeCl ₃ /chemical struvite	NO ₃ ⁻ /PO ₄ ³⁻	NA	NR	9252.45-32,383.58	(Rizzioli et al. 2023)
Ion exchange	Ion exchange membrane bioreactor (IEMB)	NO ₃ ⁻	NA	997	49,000	(Akula et al. 2024)
Biological nutrient removal (BNR)	Hydrogen-based membrane biofilm reactors	NO ₃ ⁻	NA	1808.43	1,130,271	(Cruces et al. 2023)

Abbreviations: [COP]: Colombian pesos; [NA]: not applicable; [NR]: not reported.

3.3.3 | TEA Indicator

To enable a consistent comparison of the proposed process with other studies and technologies, all economic values were normalized to COP2025. Reported values originally expressed in USD were converted to Colombian pesos using an average exchange rate of 1 USD = 4205.66 COP (2025 reference). In addition to the adsorbent production cost (COP/kg), the TEA includes the treatment cost per unit volume of wastewater (COP/m³) and the cost per unit mass of nutrient removed (COP/kg), enabling comparison across heterogeneous technologies. This approach avoids misleading interpretations based solely on adsorbent cost, which is strongly influenced by feedstock type, activation method, process scale, and system boundaries.

When compared with conventional nutrient-removal technologies, the cost of the RHB-Mg system (3,200,000 COP/kg of nutrient removed) is higher than that of biological nutrient removal processes (1,130,271 COP/kg), ion exchange–membrane systems (49,000 COP/kg), and chemical precipitation processes (9252.45–32,383.58 COP/kg).

In general, RHB-Mg for nutrient removal exhibits higher costs than other bioadsorbents and conventional treatment processes, indicating that the system is not commercially viable under the baseline scenario, particularly when operated under nonoptimized conditions and configurations with high reagent demand.

Figure 3 presents the NPV analysis for the cash flow of the proposed RHB-Mg production and application system, considering different costs of magnesium chloride. The blue line (labeled 100) represents the NPV calculated using the current market price of magnesium chloride in Colombia, which was identified as the most influential factor in the production cost of the proposed bio-adsorbent.

The figure also includes three alternative scenarios where the magnesium chloride price is reduced to 50%, 40%, and 30% of the Colombian market value, represented by red (50), green (40), and purple (30) lines, respectively.

In none of these cases did the project achieve economic feasibility within a 20-year operating period, indicating that the system is not profitable under the evaluated conditions. However, as the magnesium chloride price decreases, project feasibility improves, highlighting the critical role of reagent costs in the overall economic viability of bio-adsorbent production. This underscores the need for developing cost-effective magnesium chloride production or recovery methods within the Colombian context.

Another important factor influencing production costs is processing scale. Larger industrial facilities typically benefit from economies of scale, leading to significantly lower unit production costs (Alonso-Gómez et al. 2024).

To further explore the sensitivity of magnesium chloride pricing, two international price scenarios were evaluated (Figure 4). In Scenario 1 (P1), the magnesium chloride price was COP 1,459,267.26/t, based on quotations from Shandong Yifengtuo Chemical Co. Ltd. (China); in Scenario 2 (P2), the price was

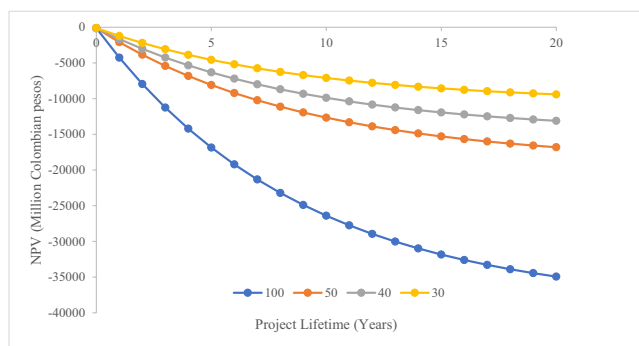


FIGURE 3 | Economic indicator (net present value) at different magnesium chloride prices. Values represent % of MgCl₂ price.

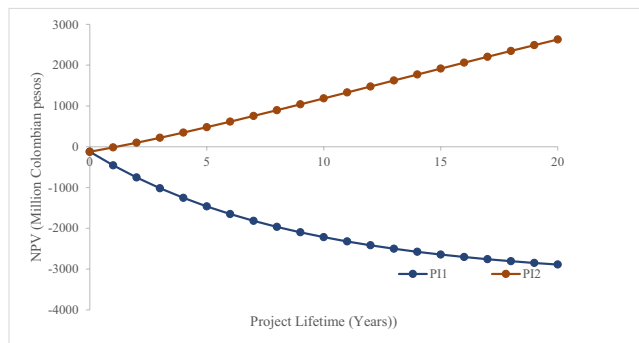


FIGURE 4 | Economic indicator (net present value) under national and international magnesium chloride price scenarios.

COP 263,680.45/t, quoted by Nanjing Jiayi Sunway Chemical Co. Ltd. (China).

Under Scenario 1, the project remained economically unfeasible, whereas in Scenario 2, it became highly profitable, recovering the initial investment within 1 to 3 years at the analyzed processing scale.

Therefore, to achieve feasibility in Colombia, a magnesium chloride price like that in Scenario 2 would be required.

A techno-economic study conducted in China by Peng et al. (2023) found that the modification of maize biochar with magnesium chloride for nutrient adsorption from livestock wastewater, followed by soil amendment, was economically viable.

However, unlike the present research, their analysis focused on total benefit rather than NPV. This finding suggests that lower reagent costs and energy prices in China make the large-scale implementation of RHB-Mg for water and soil remediation economically feasible, offering significant environmental, social, and economic benefits.

The baseline TEA was initially developed using the Colombian commercial MgCl₂ price (COP 11,783,999/t), which led to high operating costs and negative NPV values. Considering the strong influence of reagent price on the economic performance of the system, additional uncertainty and scenario analyses were performed using lower international MgCl₂ prices based

TABLE 5 | Main economic assumptions and parameters considered in the techno-economic assessment of the RHB-Mg adsorption system.

Parameter	Value	Unit
Project lifetime	20	years
Discount rate	12	%
Inflation rate	3	%
Initial capital investment (CAPEX)	122,762,675	COP
Annual treated wastewater volume	1576.8	m ³ /year
MgCl ₂ price	263,680.45	COP/ton
Annual MgCl ₂ consumption	415	ton/year
Electricity cost	1000	COP/kWh
Annual electricity consumption	28,451	kWh/year
Biochar yield	50	%
Adsorption treatment cost	2324	COP/m ³
Labor cost	25,000,000	COP/year
Maintenance cost	12,000,000	COP/year
Transport cost	8,000,000	COP/year

on Chinese industrial market quotations (reference value: COP 263,680.45/t). These alternative scenarios were included to explore the potential economic behavior of the adsorption system under more favorable large-scale supply conditions. Table 5 summarizes the main economic assumptions and parameters considered in the techno-economic assessment and uncertainty analysis of the RHB-Mg adsorption system.

The TEA results indicate that operating costs associated with reagent consumption and process operation represent the main contributors to the economic performance of the adsorption system.

Given the inherent uncertainty associated with operational costs, reagent consumption, and economic assumptions, an uncertainty and sensitivity analysis was further conducted to evaluate the robustness of the TEA results.

3.3.4 | Techno-Economic Uncertainty

To evaluate the robustness of the techno-economic assessment, a probabilistic uncertainty analysis was performed using Monte Carlo simulation combined with tornado sensitivity analysis. A total of 10,000 Monte Carlo iterations were conducted considering triangular probability distributions for the main economic parameters, including MgCl₂ price, electricity cost, biochar yield, adsorption treatment cost, labor cost, maintenance cost, transport cost, and discount rate. The selected distributions were defined using minimum, most probable, and maximum values derived from the operational assumptions adopted in the TEA.

Figure 5A presents the Monte Carlo distribution of the NPV obtained under the evaluated uncertainty conditions. The results revealed a broad NPV distribution, indicating considerable economic variability associated with the adsorption process. The probability of obtaining a positive NPV was estimated at 0%, indicating that the process is currently economically unviable under the evaluated assumptions. Even under the most optimistic price scenario (PI2), the Monte Carlo simulation still revealed a 0% probability of economic success, suggesting that the viability of the RHB-Mg system depends primarily on substantial optimization of reagent consumption rather than solely on access to lower cost international inputs. This result is consistent with the emerging and nonoptimized nature of the proposed adsorption system, where reagent consumption, operational conditions, and process scale still require substantial optimization to improve economic performance.

Figure 5B shows the tornado sensitivity analysis corresponding to a $\pm 10\%$ variation in the evaluated parameters. Among the analyzed variables, MgCl₂ price exhibited the highest influence on NPV, followed by adsorption treatment cost and operational expenditures such as labor, maintenance, and electricity consumption. In contrast, the discount rate and transport cost showed comparatively lower influence on the economic response of the system. These findings indicate that chemical consumption and operating costs are the dominant economic drivers affecting the viability of the RHB-Mg adsorption system.

Therefore, optimization of reagent usage, reduction of energy demand, and improvement of operational conditions are necessary to enhance the economic viability of the process. Overall, the present analysis should be interpreted as a preliminary techno-economic assessment intended to identify critical sources of uncertainty and sensitivity trends rather than to establish definitive commercial feasibility.

3.4 | LCA

Mg loading not only influences adsorption efficiency but also contributes to environmental impacts through reagent production and associated emissions, establishing a direct relationship between the properties of RHB-Mg and life cycle outcomes. Table 6 presents the results of the environmental assessment of the RHB-Mg application system.

Significant environmental impacts were identified in categories such as aquatic ecotoxicity (AEC), NRE use, ionizing radiation (IT), terrestrial ecotoxicity (TE), and global warming (GW).

These findings emphasize the importance of evaluating the environmental implications of each of the three process stages (Figure 6).

The RHB-Mg preparation phase was found to have the highest negative environmental impact, particularly in the categories of AEC, NRE use, IT, and GW.

This is primarily due to the high energy demand during pyrolysis, which contributes substantially to greenhouse gas emissions.

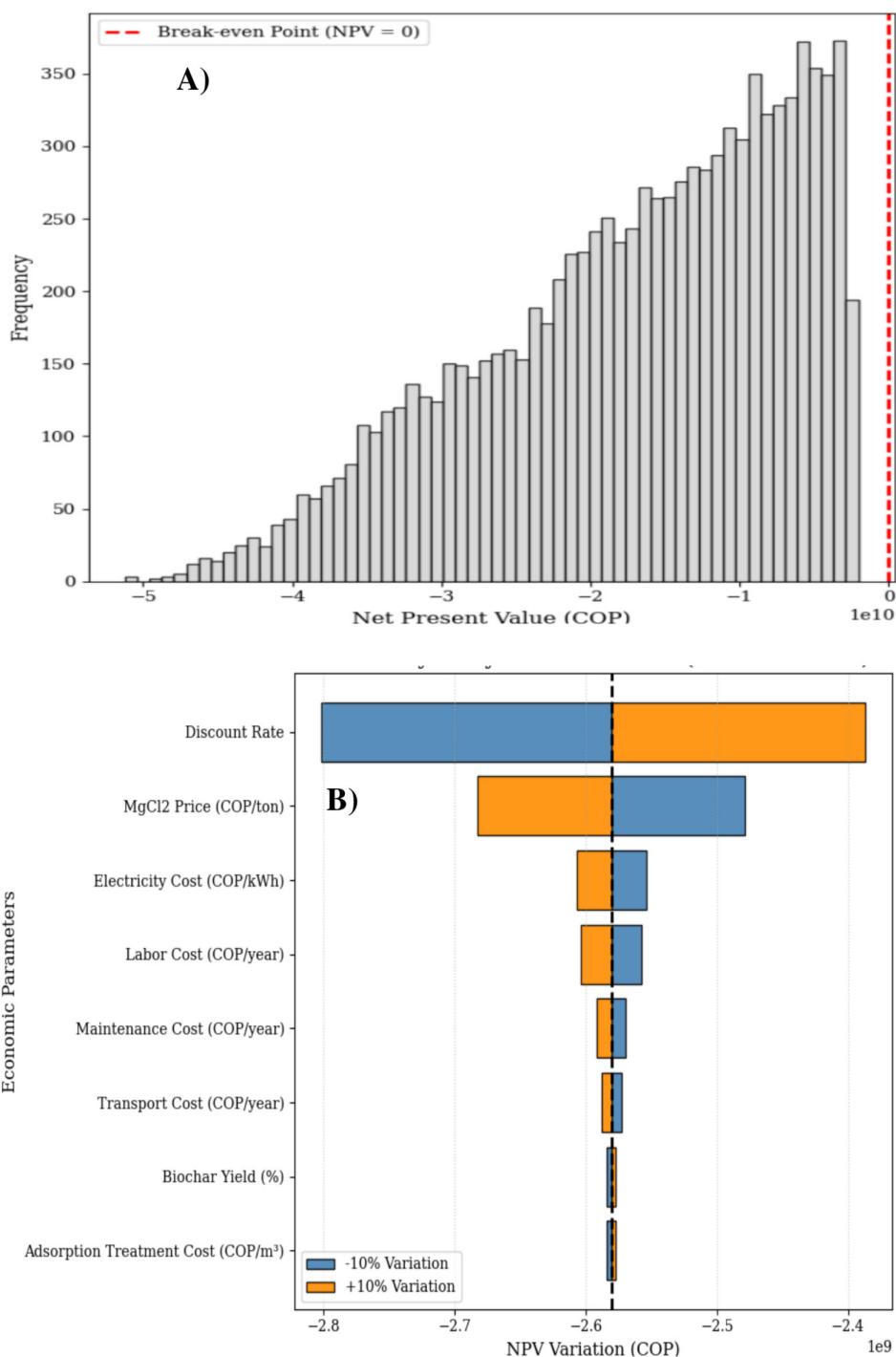


FIGURE 5 | Techno-economic uncertainty analysis of the RHB-Mg system. (A) Monte Carlo simulation showing the NPV distribution obtained from 10,000 iterations. (B) Tornado sensitivity analysis illustrating the effect of $\pm 10\%$ variation in key economic parameters on NPV.

Recovering or utilizing the energy generated during pyrolysis could help offset these negative impacts (Norberto et al. 2023).

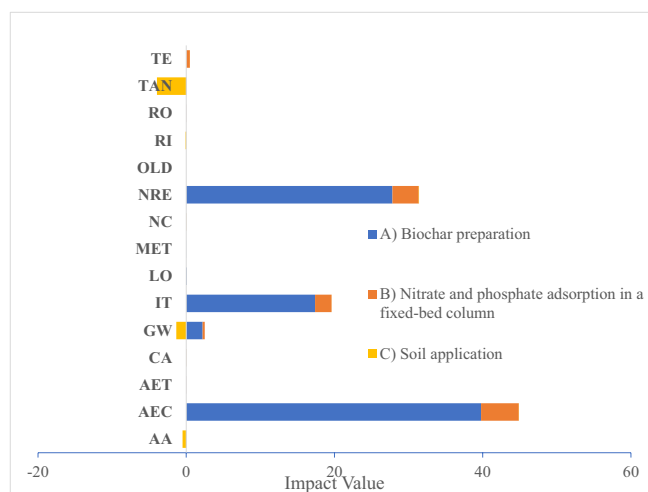
Furthermore, the use of NRE sources contributes significantly to environmental burdens; hence, substituting renewable energy sources in biochar production could mitigate the system's overall environmental impact (Norberto et al. 2023; Huang et al. 2013; Tang et al. 2020).

Conversely, the soil application phase exhibited the lowest environmental impact across all evaluated categories, showing positive contributions in terrestrial and aquatic acidification and GW mitigation (Figure 6).

These benefits can be attributed to the environmental advantages of RHB-Mg in soils, such as CO_2 sequestration, reduced N_2O emissions, lower irrigation water use, and reduced

TABLE 6 | Environmental evaluation of the overall biochar application system.

Impact category	Acronym	Unit	Value
Aquatic acidification	AA	kg SO ₂ eq	-0.49148
Aquatic ecotoxicity	AEC	kg TEG water	44.88427
Aquatic eutrophication	AET	kg PO ₄ P-lim	0.000194
Carcinogens	CA	kg C ₂ H ₃ Cl eq	0.001672
Global warming	GW	kg CO ₂ eq	1.149889
Ionizing radiation	IT	Bq C-14 eq	19.61043
Land occupation	LO	m ² org.arable	0.087495
Mineral extraction	MET	MJ surplus	5.82E-05
Noncarcinogens	NC	kg C ₂ H ₃ Cl eq	0.011842
Nonrenewable energy	NRE	MJ primary	31.41365
Ozone layer depletion	OLD	kg CFC-11 eq	1.78E-07
Respiratory inorganics	RI	kg PM2.5 eq	-0.09034
Respiratory organics	RO	kg C ₂ H ₄ eq	0.000209
Terrestrial eutrophication/nitrification	TAN	kg SO ₂ eq	-3.91711
Terrestrial ecotoxicity	TE	kg TEG soil	4.305248

**FIGURE 6** | Impacts by stages of the biochar application system.

dependence on synthetic fertilizers (Yang et al. 2021; Marzeddu et al. 2021; Zhu et al. 2022).

By decreasing the inputs required along the agricultural production chain, biochar application can lower environmental impacts while improving crop productivity.

Thus, the use of spent RHB-Mg (after adsorption) as a soil amendment can be considered a sustainable strategy for mitigating the environmental impacts associated with poor management of agro-industrial residues.

This circular approach not only reduces waste but also provides net environmental benefits due to the negative impact values achieved in several categories. However, the effectiveness of RHB-Mg when used as a soil amendment depends on nutrient retention capacity, release dynamics, and potential leaching behavior. These factors were not experimentally evaluated in this study and therefore introduce uncertainty into the system-level assessment.

In this study, it was found that applying 1 kg of RHB-Mg to soil may result in a potential climate change benefit of -1.34-kg CO₂ eq in the GW category (assuming carbon stability in soil), which is comparable to the ranges reported in previous studies (-0.07 to -1.25-kg CO₂ eq) (Norberto et al. 2023).

Other studies have reported even higher reductions (up to -6.89-kg CO₂ eq) (Moreira et al. 2017), which may be attributed to differences in biochar feedstocks, preparation methods, and field application conditions.

However, the climate change benefit associated with the application of RHB-Mg should be interpreted with caution. The reported value (-1.34-kg CO₂ eq/kg) represents a potential climate benefit derived from life cycle modeling assumptions, rather than a confirmed carbon sequestration outcome. In this study, key parameters required to assess carbon stability—such as elemental carbon content, ash content, H/Corg and O/Corg ratios, and the recalcitrant carbon fraction—were not experimentally determined.

Therefore, the estimated CO₂ reduction is subject to significant uncertainty and depends on assumptions regarding carbon permanence in soil. Previous studies have shown that carbon removal through biochar systems is strongly influenced by feedstock characteristics, pyrolysis conditions, the fraction of stable carbon, its permanence, and the system boundaries considered (Lefebvre et al. 2023; Fawzy et al. 2022).

Positive environmental outcomes were also observed for terrestrial and aquatic acidification, with respective reductions of -3.95-kg SO₂ eq and -0.5-kg SO₂ eq.

These improvements are linked to biochar's capacity to retain soil moisture thus reducing irrigation frequency and to lower fertilizer inputs, which prevents the release of acidifying substances into soil and water systems (Yang et al. 2021; Marzeddu et al. 2021; Zhu et al. 2022).

Regarding respiratory inorganic impacts, a reduction of -0.1 -kg $\text{PM}_{2.5}$ eq was estimated, associated with the decreased use of nitrogen fertilizers (Frazier et al. 2015). This outcome also contributes to a reduction in respiratory health risks in humans (Erison et al. 2022), confirming the wide range of environmental and health cobenefits that biochar application can provide.

In addition, the environmental impacts were normalized with respect to the adsorption process performance, as described in Section 2.3.1, in order to improve comparability with wastewater treatment technologies. Based on the functional unit of 1 kg of RHB-Mg, the system treats 0.03789 m^3 of wastewater, removing 0.000372 kg of NO_3^- and 0.000213 kg of PO_4^{3-} per kg of RHB-Mg.

Using the GW potential of the entire system (including RHB-Mg preparation, adsorption, and soil application), estimated at 1.149889 -kg CO_2 eq per kg of RHB-Mg, the impacts correspond to 30.35 -kg CO_2 eq per m^3 of treated wastewater, 3092.6 -kg CO_2 eq per kg of NO_3^- removed, and 5408.3 -kg CO_2 eq per kg of PO_4^{3-} removed. These results indicate that the environmental intensity of the system is mainly driven by the production of RHB-Mg, particularly by energy demand and MgCl_2 consumption. Although these values are higher than those typically reported for conventional wastewater treatment systems (Osman, Elgarahy, et al. 2022; Osman et al. 2024), they are associated with the current nonoptimized operating conditions and do not account for the potential benefits related to nutrient recovery and the reuse of spent biochar as a soil amendment.

3.4.1 | Sensitivity Analysis Comparing Different Energy Sources

The results in Figure 7 show significant differences among the three energy sources (hydroelectric, wind, and syngas) across different environmental impact categories. Hydroelectric power had the greatest impact on NRE, IT, GW, and AEC. These impacts can be attributed to the infrastructure, materials, and

energy consumption required for this kind of electricity generation. Hydroelectric power also contributed significantly to TE and to human toxicity categories, including carcinogens (CA) and noncarcinogens (NC).

Wind power consistently showed the lowest environmental impacts in most evaluated categories. This was especially true for GW, NRE, IT, aquatic and TE, and ozone layer depletion (OLD). Wind power even showed negative values in categories such as GW and ocean acidification. This suggests there may be environmental benefits from replacing conventional energy sources. These results position wind energy as the alternative with the best environmental performance in the sensitivity analysis.

Syngas showed intermediate performance between hydroelectric and wind energy. It had lower impacts than hydroelectric energy in most categories, but its environmental contributions remain relevant in AEC, NRE, and TE. The use of biomass-derived synthesis gas is promising. It can valorize agro-industrial waste and reduce dependence on fossil fuels.

Overall, the sensitivity analysis indicates that wind energy is the most environmentally sustainable option, while hydroelectric energy exhibited the greatest impacts in several evaluated categories. Syngas, for its part, showed a favorable environmental performance compared to hydroelectric energy, although it still requires optimization to reduce impacts associated with thermochemical processes and resource consumption. These results suggest that integrating alternative renewable sources, particularly wind energy and biomass-based syngas, could help reduce the environmental impacts of biochar production and utilization systems in Colombia.

4 | Perspectives and Future Work

This study provides a system-level evaluation of RHB-Mg for the removal of nitrates and phosphates from wastewater

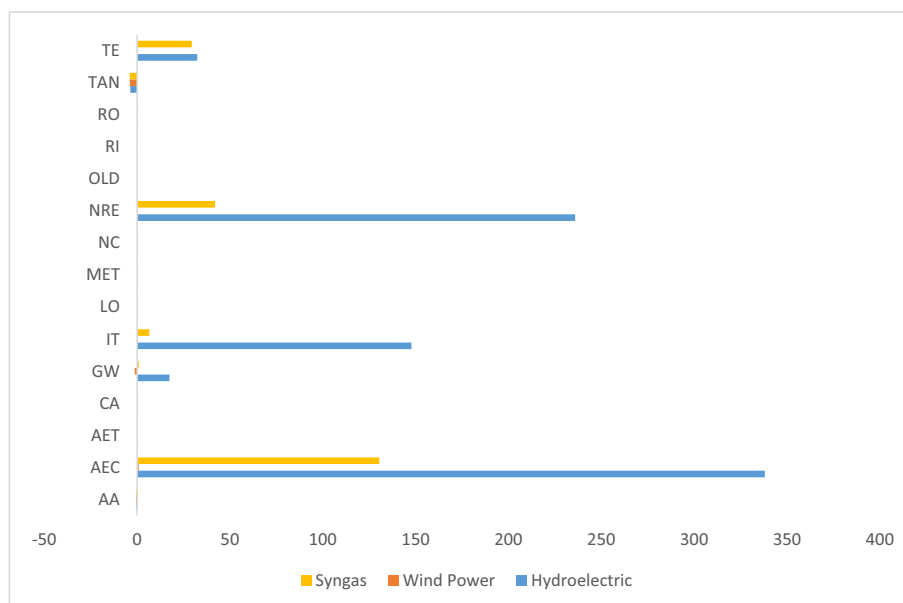


FIGURE 7 | Sensitivity analysis of the type of energy used. The units for the impact category have been specified above (Table 6).

based on fixed-bed column adsorption data. Detailed adsorption metrics such as breakthrough curve integration and adsorption capacity (mg/g) were not recalculated in this study, as they were previously reported in the experimental work on which this analysis is based. However, several aspects require further investigation to support its practical implementation at larger scales.

In particular, experimental validation at pilot scale is needed to confirm the assumptions used in the scale-up analysis and to evaluate long-term operational stability under realistic conditions. Factors such as mass transfer limitations, pressure drop, and continuous operation performance should be examined in more detail.

Process optimization also remains a key area for future work. The results indicate that magnesium chloride consumption is a major contributor to operational costs, and therefore strategies aimed at reducing reagent use and improving energy efficiency are essential to enhance the overall economic feasibility of the system.

In other hand, future research should include a detailed Mg and chloride mass balance across all process stages, including impregnation, washing, adsorption, and soil application. This should involve quantification of Mg retention efficiency, characterization of washing effluents, and evaluation of potential Mg and chloride leaching under operational and environmental conditions.

From a circular-economy perspective, future studies should also consider the reuse of treated wastewater (e.g., for irrigation), which was not addressed in the present work but could further strengthen the integrated nature of the proposed approach.

Similarly, the agricultural application of nutrient-loaded biochar should be validated through controlled soil experiments to better understand nutrient availability, crop response, and potential environmental impacts, particularly under long-term conditions.

In addition, further characterization of the spent RHB-Mg is required to assess its suitability for soil application, including the evaluation of possible contaminant accumulation, magnesium and chloride release, and overall material safety.

Finally, the absence of post-adsorption characterization represents a limitation of this study, especially in relation to confirming the mechanisms governing nitrate removal. Future research should also incorporate uncertainty and sensitivity analyses to improve the robustness of techno-economic and environmental assessments.

5 | Conclusions

The scaling of the adsorption process and the estimation of RHB-Mg requirements for its sequential use as an adsorbent in fixed-bed columns and as a soil amendment provide a

preliminary assessment of the system. Based on these results, an integrated evaluation of the economic and environmental performance of the RHB-Mg production and application system was developed. Overall, this study presents a system-level analysis, and further experimental validation at pilot scale is required prior to practical implementation.

The results indicate that, although the system offers potential environmental and circular-economy benefits, its economic feasibility is currently constrained by the high consumption of magnesium chloride. This parameter should be interpreted as a nonoptimized design condition and represents a critical lever for improving both economic and environmental performance. In this context, optimization of MgCl₂ dosage while maintaining adsorption efficiency emerges as a key priority for future research.

From an environmental perspective, the most sustainable stage of the evaluated system corresponds to the application of spent RHB-Mg to soil, whereas the biochar production stage exhibited the lowest performance, with negative impacts in categories such as AEC, IT, and NRE use. These findings highlight the need for mitigation strategies, including improved energy recovery and the incorporation of renewable energy sources during pyrolysis.

The economic analysis further confirms that magnesium chloride consumption is the dominant cost driver and has a decisive influence on overall feasibility. Under current Colombian market conditions, the system is not economically viable; however, scenarios considering lower reagent prices suggest that implementation could become feasible. This underscores the importance of both reducing reagent consumption and exploring alternative supply strategies.

The soil application stage was evaluated as a prospective scenario based on literature data and LCA, rather than direct experimental validation. Therefore, future work should prioritize field-scale studies to validate the agronomic performance and environmental benefits of nutrient-enriched RHB-Mg under real conditions. In addition, further research should address the development of a detailed mass balance of Mg and chloride, including retention, losses during washing, and potential leaching, as well as the long-term stability of RHB-Mg (e.g., H/C ratio) to confirm its suitability for soil application.

The climate change benefits associated with RHB-Mg application are subject to significant uncertainty, particularly due to assumptions regarding carbon stability and permanence in soil. Therefore, the reported CO₂ reduction should be interpreted as a potential outcome rather than a confirmed carbon sequestration effect.

Finally, future studies should focus on optimizing process conditions—particularly reducing MgCl₂ consumption during impregnation—to enhance the operational efficiency and competitiveness of the system. Comparative assessments with conventional nutrient removal technologies will also be necessary to fully establish the practical advantages of RHB-Mg-based approaches.

Author Contributions

Elkyn Lugo-Arias: writing – review and editing, supervision. **Jose Villa-Parejo:** methodology, supervision, writing – review and editing. **Guido Escorcía:** writing – review and editing, software. **José Lugo-Arias:** conceptualization, methodology, writing – original draft. **Sandra Vargas:** writing – review and editing, supervision, methodology. **Julia González-Álvarez:** supervision, writing – review and editing.

Acknowledgments

The authors thank the Universidad del Magdalena (Santa Marta, Magdalena, Colombia) and Ministerio de Ciencia, Tecnología e Innovación (Colombia).

Funding

This work was supported by the Universidad del Magdalena.

Conflicts of Interest

The authors declare no conflicts of interest.

Data Availability Statement

All relevant data are included in the paper or in the [Supporting Information](#).

Consent

All authors agreed to submit this research for publication.

References

- Akula, V. V., G. Ramalingam, A. K. Verma, et al. 2024. “Performance Evaluation of Pilot Scale Ion Exchange Membrane Bioreactor for Nitrate Removal From Secondary Effluent.” *Journal of Cleaner Production* 442: 141087.
- Alonso-Gómez, L. A., D. D. Celis-Carmona, Y. F. Rodríguez-Sánchez, J. R. Castro-Ladino, and J. C. Solarte-Toro. 2024. “Biochar Production From Cassava Waste Biomass: A Techno-Economic Development Approach in the Colombian Context.” *Bioresource Technology Reports* 26: 101872.
- Banerjee, S., S. Mukherjee, A. LaminKa-ot, S. R. Joshi, T. Mandal, and G. Halder. 2016. “Biosorptive Uptake of Fe²⁺, Cu²⁺ and As⁵⁺ by Activated Biochar Derived From *Colocasia esculenta*: Isotherm, Kinetics, Thermodynamics, and Cost Estimation.” *Journal of Advanced Research* 7: 597–610.
- Bian, H., M. Wang, J. Huang, et al. 2024. “Large Particle Size Boosting the Engineering Application Potential of Functional Biochar in Ammonia Nitrogen and Phosphorus Removal From Biogas Slurry.” *Journal of Water Process Engineering* 57: 104640.
- Biswas, B., S. Adhikari, H. Jahromi, et al. 2024. “Magnesium Doped Biochar for Simultaneous Adsorption of Phosphate and Nitrogen Ions From Aqueous Solution.” *Chemosphere* 358: 142130.
- Blanco-Canqui, H. 2017. “Biochar and Soil Physical Properties.” *Soil Science Society of America Journal* 81: 687–711.
- Chen, M., Y. Liu, J. Pan, Y. Jiang, X. Zou, and Y. Wang. 2024. “Low-Cost Ca/Mg Co-Modified Biochar for Effective Phosphorus Recovery: Adsorption Mechanisms, Resourceful Utilization, and Life Cycle Assessment.” *Chemical Engineering Journal* 502: 157993.
- Cruces, M., J. Suárez, I. Nancucheo, and A. Schwarz. 2023. “Optimization of the Chemolithotrophic Denitrification of Ion Exchange Concentrate

Using Hydrogen-Based Membrane Biofilm Reactors.” *Journal of Environmental Management* 348: 119283.

El-Azazy, M., I. Nabil, S. S. Hassan, and A. S. El-Shafie. 2021. “Adsorption Characteristics of Pristine and Magnetic Olive Stones Biochar With Respect to Clofazimine.” *Nanomaterials* 11: 963.

El-Shafie, A. S., E. Rahman, Y. Gadelhak, R. Mahmoud, and M. El-Azazy. 2024. “Techno-Economic Assessment of Waste Mandarin Biochar as a Green Adsorbent for Binary Dye Wastewater Effluents of Methylene Blue and Basic Fuchsin: Lab- and Large-Scale Investigations.” *Spectrochimica Acta. Part A, Molecular and Biomolecular Spectroscopy* 306: 123621.

Erison, A. E. a., Y. H. Tan, N. M. Mubarak, et al. 2022. “Life Cycle Assessment of Biodiesel Production by Using Impregnated Magnetic Biochar Derived From Waste Palm Kernel Shell.” *Environmental Research* 214: 114149.

Esmati, F., M. C. Holliday, S. H. Zein, K. J. Jabbar, S. H. Tan, and A. Putranto. 2024. “Enhancing Hexavalent Chromium Removal From Textile Effluent With Low-Cost Adsorbent: Simulation and a Techno-Economic Study.” *International Journal of Environmental Science and Technology* 22: 6345–6364.

Fang, C., T. Zhang, P. Li, R. F. Jiang, and Y. C. Wang. 2014. “Application of Magnesium Modified Corn Biochar for Phosphorus Removal and Recovery From Swine Wastewater.” *International Journal of Environmental Research and Public Health* 11: 9217–9237.

Fawzy, S., A. I. Osman, N. Mehta, D. Moran, A. H. Al-Muhtaseb, and D. W. Rooney. 2022. “Atmospheric Carbon Removal via Industrial Biochar Systems: A Techno-Economic-Environmental Study.” *Journal of Cleaner Production* 371: 133660.

Frazier, R., E. Jin, and A. Kumar. 2015. “Life Cycle Assessment of Biochar Versus Metal Catalysts Used in Syngas Cleaning.” *Energies (Basel)* 8: 621–644.

Gariya, D., and B. Satyavathi. 2024. “Designer Biochar With Specific Functionalities for the Sustainable Mining of Invaluable Metals From Sea Water: Performance Assessment, Mechanism Insights and Cost Benefit Analysis.” *Chemical Engineering Journal* 479: 147334.

Gopalakrishnan, Y., A. Al-Gheethi, M. Abdul Malek, et al. 2020. “Removal of Basic Brown 16 From Aqueous Solution Using Durian Shell Adsorbent, Optimisation and Techno-Economic Analysis.” *Sustainability* 12: 8928.

Huang, Y.-F., F.-S. Syu, P.-T. Chiueh, and S.-L. Lo. 2013. “Life Cycle Assessment of Biochar Cofiring With Coal.” *Bioresource Technology* 131: 166–171.

Iamsaard, K., C. H. Weng, J. H. Tzeng, J. Anotai, A. R. Jacobson, and Y. T. Lin. 2023. “Systematic Optimization of Biochars Derived From Corn Wastes, Pineapple Leaf, and Sugarcane Bagasse for Cu(II) Adsorption Through Response Surface Methodology.” *Bioresource Technology* 382: 129131.

Ighalo, J. O., F. O. Omoarukhe, V. E. Ojukwu, K. O. Iwuzor, and C. A. Igwegbe. 2022. “Cost of Adsorbent Preparation and Usage in Wastewater Treatment: A Review.” *Cleaner Chemical Engineering* 3: 100042.

Jellali, S., S. Hadroug, M. Al-Wardy, et al. 2024. “Phosphorus Recovery From Aqueous Solutions by a Mg/Al-Modified Biochar From Date Palm Wastes in Column Mode: Adsorption Characteristics and Scale-Up Design Parameters Assessment.” *Biomass Conversion and Biorefinery* 15: 27437–27452.

Jiang, Y. H., A. Y. Li, H. Deng, et al. 2019. “Characteristics of Nitrogen and Phosphorus Adsorption by Mg-Loaded Biochar From Different Feedstocks.” *Bioresource Technology* 276: 183–189.

Jolliet, O., M. Margni, R. Charles, et al. 2003. “IMPACT 2002+: A New Life Cycle Impact Assessment Methodology.” *International Journal of Life Cycle Assessment* 8: 324.

- Jung, K.-W., T.-U. Jeong, J.-W. Choi, K.-H. Ahn, and S.-H. Lee. 2017. "Adsorption of Phosphate From Aqueous Solution Using Electrochemically Modified Biochar Calcium-Alginate Beads: Batch and Fixed-Bed Column Performance." *Bioresource Technology* 244: 23–32.
- Kumar, P. S., L. Korving, M. C. M. van Loosdrecht, and G.-J. Witkamp. 2019. "Adsorption as a Technology to Achieve Ultra-Low Concentrations of Phosphate: Research Gaps and Economic Analysis." *Water Research X* 4: 100029.
- Lefebvre, D., S. Fawzy, C. A. Aquije, A. I. Osman, K. T. Draper, and T. A. Trabold. 2023. "Biomass Residue to Carbon Dioxide Removal: Quantifying the Global Impact of Biochar." *Biochar* 5: 65.
- Liu, X., W. Zhou, L. Feng, L. Wu, J. Lv, and W. Du. 2022. "Characteristics and Mechanisms of Phosphorous Adsorption by Peanut Shell-Derived Biochar Modified With Magnesium Chloride by Ultrasonic-Assisted Impregnation." *ACS Omega* 7: 43102–43110.
- Lugo-Arias, J., J. González-Álvarez, and A. Maturana. 2026. "Mg-Impregnated Rice Husk Biochar in Fixed-Bed Columns: High-Capacity Continuous-Flow Removal of Nitrate and Phosphate From Wastewater." *Biomass Conversion and Biorefinery* 16: 149.
- Lugo-Arias, J., J. González-Álvarez, A. Maturana, J. Villa-Parejo, and C. Barraza-Heras. 2025. "Removal of Nitrate and Phosphate From Aqueous Solutions Using Bioadsorbents Derived From Agro-Industrial Wastes of Rice Husk and Corn Stalk." *Biomass Conversion and Biorefinery* 15: 19453–19475.
- Lugo-Arias, J., J. Villa-Parejo, G. Escorcia, et al. 2025. "Life Cycle Assessment of Magnesium-Impregnated Biochar Production and Its Application for Nutrient Removal and Soil Improvement in Rice Cultivation." *Advanced Sustainable Systems* 9: 9.
- Marzeddu, S., A. Cappelli, A. Ambrosio, M. A. Décima, P. Viotti, and M. R. Boni. 2021. "A Life Cycle Assessment of an Energy-Biochar Chain Involving a Gasification Plant in Italy." *Land (Basel)* 10: 1256.
- Mohammadi, A., A. Cowie, T. L. Anh Mai, et al. 2016. "Biochar Use for Climate-Change Mitigation in Rice Cropping Systems." *Journal of Cleaner Production* 116: 61–70.
- Moreira, M. T., I. Noya, and G. Feijoo. 2017. "The Prospective Use of Biochar as Adsorption Matrix—A Review From a Lifecycle Perspective." *Bioresource Technology* 246: 135–141.
- Norberto, J., K. Zoroufchi Benis, K. N. McPhedran, J. Soltan, and J. Environ. 2023. "Microwave Activated and Iron Engineered Biochar for Arsenic Adsorption: Life Cycle Assessment and Cost Analysis." *Chemical Engineer* 11: 109904.
- Osman, A. I., A. M. Elgarahy, N. Mehta, et al. 2022. "Facile Synthesis and Life Cycle Assessment of Highly Active Magnetic Sorbent Composite Derived From Mixed Plastic and Biomass Waste for Water Remediation." *Chemical Engineer* 10: 12433–12447.
- Osman, A. I., M. Farghali, and A. K. Rashwan. 2024. "Life Cycle Assessment of Biochar as a Green Sorbent for Soil Remediation." *Current Opinion in Green and Sustainable Chemistry* 46: 100882.
- Osman, A. I., S. Fawzy, M. Farghali, et al. 2022. "Biochar for Agronomy, Animal Farming, Anaerobic Digestion, Composting, Water Treatment, Soil Remediation, Construction, Energy Storage, and Carbon Sequestration: A Review." *Environmental Chemistry Letters* 20: 2385–2485.
- Patel, M. R., and N. L. Panwar. 2024. "Evaluating the Agronomic and Economic Viability of Biochar in Sustainable Crop Production." *Biomass Bioenergy* 188: 107328.
- Peng, Y., Y. Luo, Y. Li, et al. 2023. "Effect of Corn Pre-Puffing on the Efficiency of MgO-Engineered Biochar for Phosphorus Recovery From Livestock Wastewater: Mechanistic Investigations and Cost Benefit Analyses." *Biochar* 5: 26.
- Pratiwi, E. P. A., A. K. Hillary, T. Fukuda, and Y. Shinogi. 2016. "The Effects of Rice Husk Char on Ammonium, Nitrate and Phosphate Retention and Leaching in Loamy Soil." *Geoderma* 277: 61–68.
- Praveen, S., R. Gokulan, T. B. Pushpa, and J. Jegan. 2021. "Techno-Economic Feasibility of Biochar as Biosorbent for Basic Dye Sequestration." *Journal of the Indian Chemical Society* 98: 100107.
- Rajabi Hamedani, S., T. Kuppens, R. Malina, E. Bocci, A. Colantoni, and M. Villarini. 2019. "Life Cycle Assessment and Environmental Valuation of Biochar Production: Two Case Studies in Belgium." *Energies (Basel)* 12: 2166.
- Rizzioli, F., D. Bertasini, D. Bolzonella, N. Frison, and F. Battista. 2023. "A Critical Review on the Techno-Economic Feasibility of Nutrients Recovery From Anaerobic Digestate in the Agricultural Sector." *Separation and Purification Technology* 306: 122690.
- Saldarriaga, J. 2016. *Hidráulica de Tuberías, Abastecimiento de Agua, Redes, Riegos*. Alfaomega.
- Seow, Y. X., Y. H. Tan, J. Kandedo, et al. 2024. "Pyrolysis Assessment of Palm Kernel Shell Waste Valorization to Sulfonated Magnetic Biochar From Techno-Economic and Energy Perspectives." *Discover Applied Sciences* 6: 398.
- Sivaraman, S., T. Subramaniam, S. R. Shanmugam, D. Sappani, P. Venkatachalam, and N. M. C. Saady. 2024. "Valorization of Prosopis Juliflora Biochar for Supercapacitor Application: Techno-Economic and Lifecycle Analysis." *Journal of Cleaner Production* 471: 143409.
- Tang, Y., J. Dong, G. Li, et al. 2020. "Environmental and Exergetic Life Cycle Assessment of Incineration- and Gasification-Based Waste to Energy Systems in China." *Energy* 205: 118002.
- Tran, D. T., T. D. Pham, V. C. Dang, et al. 2022. "A Facile Technique to Prepare MgO-Biochar Nanocomposites for Cationic and Anionic Nutrient Removal." *Journal of Water Process Engineering* 47: 102702.
- Yang, Q., O. Mašek, L. Zhao, et al. 2021. "Country-Level Potential of Carbon Sequestration and Environmental Benefits by Utilizing Crop Residues for Biochar Implementation." *Applied Energy* 282: 116275.
- Zhang, X., Y. Xiong, X. Wang, et al. 2024. "MgO-Modified Biochar by Modifying Hydroxyl and Amino Groups for Selective Phosphate Removal: Insight Into Phosphate Selectivity Adsorption Mechanism Through Experimental and Theoretical." *Science of the Total Environment* 918: 170571.
- Zhu, X., C. Labianca, M. He, et al. 2022. "Life-Cycle Assessment of Pyrolysis Processes for Sustainable Production of Biochar From Agro-Residues." *Bioresource Technology* 360: 127601.

Supporting Information

Additional supporting information can be found online in the Supporting Information section. **Table S1:** Summary of small-scale fixed-bed column adsorption data **Table S2:** Design parameters for scaling the nitrate and phosphate removal process **Table S3:** Design parameters for scaling the pyrolysis process **Table S4:** Design parameters for scaling the biochar soil application process